Measuring Atmospheric Turbulence with Airborne Hot-Film Anemometers

FRANCIS J. MERCERET

National Hurricane and Experimental Meteorology Laboratory, NOAA, Coral Gables, Fla. 33124

(Manuscript received 31 July 1975, in revised form 1 March 1976)

ABSTRACT

Extensive flight tests during GATE showed hot-film anemometry to be a useful tool for the airborne measurement of atmospheric turbulence in clear air and in subcloud rain, but not within clouds. Root-mean-square noise values lower than 0.08 m s^{-1} for velocity and 0.03°C for temperature were obtained over the scale range of 50 m to 4 cm at altitudes from 16 to 2000 m. Spectra of U', W' and θ were obtained over the same range with roughly 1 dB accuracy. Dissipation rates could be determined to within ±30%. Cross-component contamination was too large to permit reliable cross spectra to be obtained. It is suggested that an upgraded system could significantly reduce such contamination and improve the overall accuracy and signal-to-noise ratio.

1. Introduction

Hot-sensor anemometry has been the principal tool for laboratory measurements of turbulence. The literature on the subject is extensive and the foundations have been carefully presented by several writers, including Corrsin (1963), Hinze (1959) and Kovasznay (1965). Hot wires have also been used for more than a decade in the atmosphere, especially for air-sea interaction studies where their high-frequency response is required (e.g., Pond *et al.*, 1963). Because hot wires are fragile, however, they have nearly always been limited to use on surface platforms rather than aircraft, thus severely restricting the portion of the atmosphere that they have sampled.

Laboratory tests suggested the possibility that airborne hot-film anemometers, which are much more rugged than hot-wire anemometers, might function adequately even during heavy rain (Merceret, 1970). Their utility in a maritime environment was demonstrated by Dorman and Mollo-Christensen (1973), while the feasibility of using fragile hot wires on aircraft was shown by Chernikov *et al.* (1969) and Sheih *et al.* (1971). During the GARP Atlantic Tropical Experiment (GATE) (June–September, 1974), three channels of constant temperature hot-film anemometry were operated aboard the NOAA Research Flight Facility (RFF) DC-6 aircraft in wet and dry environments from the surface (16 m) to altitudes as great as 2000 m. This paper describes the system and evaluates its operation in these environments.

2. The hot-film installation

Fig. 1 is a diagram of the National Hurricane Research Laboratory GATE turbulence system. The system comprises three DISA 55D05 constant temperature anemometers[1] operated in the 1:1 bridge ratio with accessory ac power supplies, a level shifter and prewhitener

[1] The mention of a proprietary product does not constitute an endorsement thereof by the author or the National Hurricane and Experimental Meteorology Laboratory and no reference implying such endorsement shall be made to this paper in any promotion or advertisement.

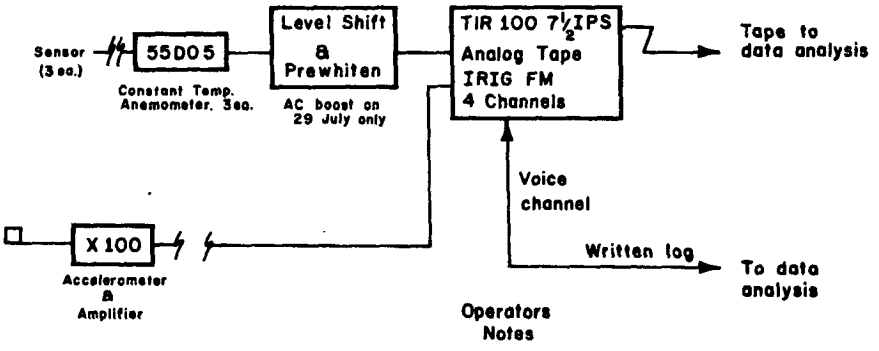

FIG. 1. Diagram of the NHRL hot-film turbulence measurement system.

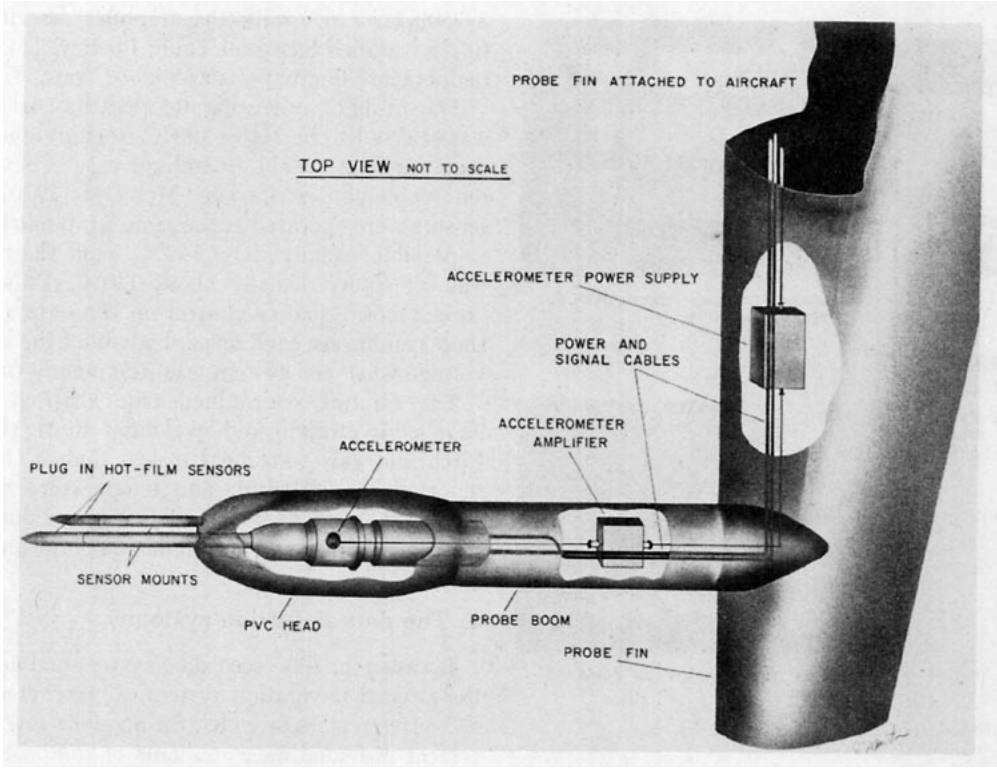

FIG. 2. Turbulence probe head and mounting boom diagram showing location of sensors and boom electronics.

constructed in the laboratory, a Tandberg model TIR-100, four-channel FM-IRIG analog tape recorder operated at $7\frac{1}{2}$ inches per second, and a composite, four-sensor probe head. The probe head comprises a Bolt, Beranek and Newman model 501 miniature accelerometer and home-made amplifier to measure vibration of the probe head, a DISA 55A81 single-sensor hot-film probe, and a DISA 55A89 dual sensor hot-film probe. Fig. 2 shows the construction of the probe head and mount.

Whenever possible, we have used readily available commercial equipment in the configuration recommended by the manufacturer. Maximum use of the recorder's dynamic range was attained by prewhitening and level shifting, but otherwise the system is a simple connection of stock items.

The dual sensor "V-probe" was used to resolve the streamwise and normal (nominally vertical) velocity components (Champagne and Sleicher, 1967), while the third hot film enabled the temperature fluctuations to be recovered. The accelerometer was included to measure the vibration velocity of the sensors and remove it, if necessary, from the normal component. The mount is so rigid that no accelerometer was needed for measuring streamwise vibrations. The geometry of the sensors is shown in Fig. 3. The entire system as installed on the DC-6 is presented in Fig. 4.

3. Calibrating and operating the anemometers

The anemometers were calibrated in a low-turbulence wind tunnel at the School of Engineering and Environmental Design of the University of Miami. Typical calibrations are shown in Fig. 5. Every probe was individually calibrated, and each obeyed the classical hot-wire equation

$$E^2 R^{-1} = (A + BU^N)(T_s - T_a), \qquad (1)$$

usually called King's law, where E, R and T_s are respectively the voltage drop, resistance, and temperature of the sensor, T_a is the ambient flow temperature, U the component of the flow velocity normal to the sensor, and A, B and N are King's law constants. For

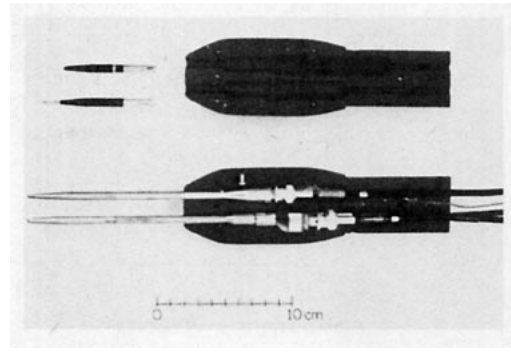

FIG. 3. The geometry of the sensing head.

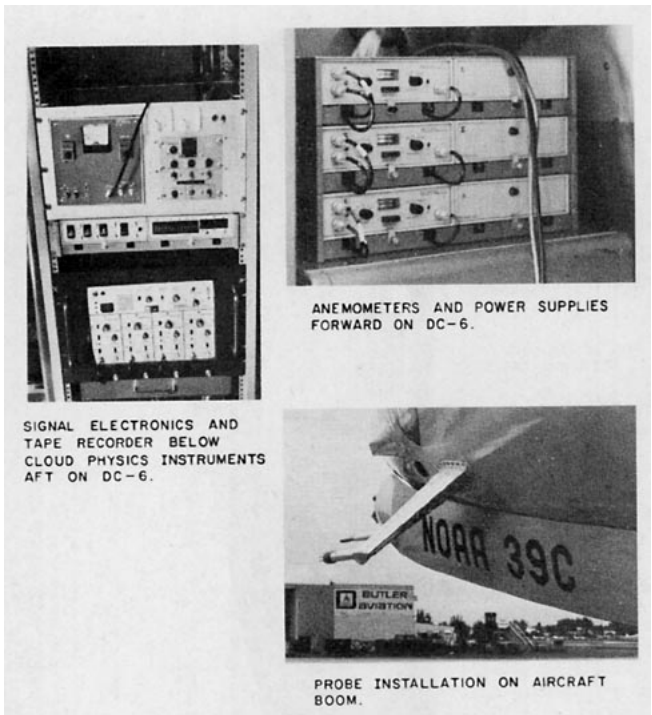

FIG. 4. The installation on the DC-6.

all of our probes, $N=\frac{1}{3}$, a value typical for wedge-shaped hot films as distinguished from cylindrical shapes for which $N=\frac{1}{2}$. Values of A and B differed, but typically $A\approx 4\times10^{-4}$ W C^{-1} and $B\approx 1.7\times10^{-4}$ W (m s^{-1})$^{-\frac{1}{3}}$ C^{-1}. The accuracy and resolution of the system are limited by the electronic noise in the equipment, and with the operating conditions described below, the limit of reliable measurements is ± 3 cm s^{-1} at $U=100$ m s^{-1} under laboratory conditions. Worst case system output noise values in flight were 0.020 V rms. This is equivalent to velocity fluctuations of <0.08 m s^{-1} rms in the 2–2500 Hz range with the amplifier described in Section 5 installed based on Table 1 below. The equivalent temperature fluctuations are 0.03°C rms.

The in-flight operating temperature of the sensors was selected to be above 100°C to guarantee that raindrop impacts would unambiguously identifiable and removable as described by Merceret (1970). The dual sensors were operated at the same temperature as nearly as possible, usually about 140°C, while the single sensor was set cooler, usually about 110°C. This facilitated "quick-look" quality control on the data since, under these conditions, each sensor had about the same output voltage when the system was functioning properly.

The aircraft maintained true airspeed of roughly 92 m s^{-1} in straight and level flight during the data legs. Pitch and yaw were held to less than 3° for the data reported here. Altitude and temperature ranged from 16 m at 27°C to 2000 m at 14°C. These values define the envelope of operating environments of the anemometers.

4. The data reduction system

Because the data recording system had no tie-in with the aircraft navigation system, we restricted our analysis to frequencies at which the accelerometer within our system provided measurements of the probe head motion so that the velocity data could be referred to an inertial reference frame. The frequency range was also restricted by the bandwidth of the tape recorder. These restrictions limited measurements to the region from 2 to 2500 Hz, corresponding roughly to scales from 50 m to 4 cm. We assumed that vibrations of the probes along the flight axis at these frequencies were much smaller than those we measured normal to it. This assumption is supported by the measurements of Brown *et al.* (1974), which show that except for discrete frequencies associated with engine and airframe vibra-

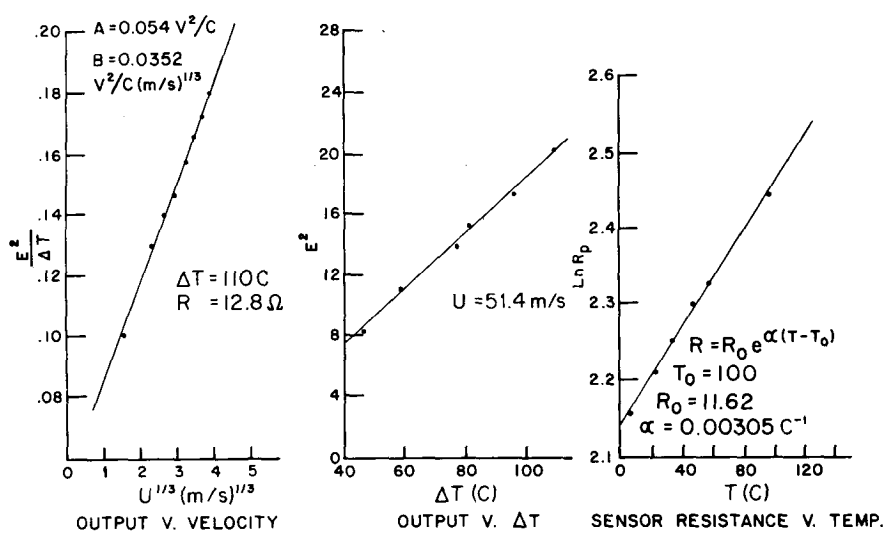

FIG. 5. Typical King's law calibrations.

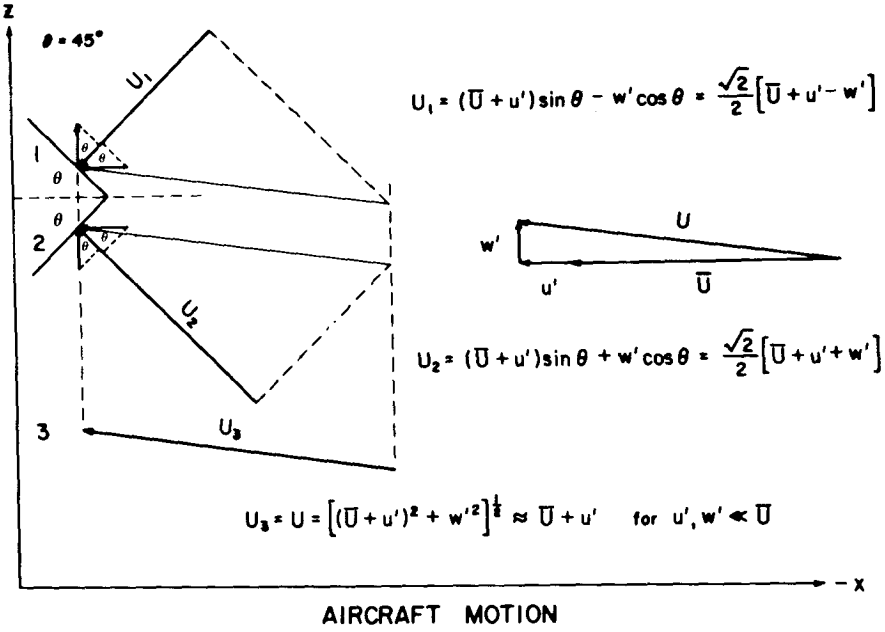

FIG. 6. Diagram of the configuration of the hot-film sensors and the flow field.

tion, high-frequency motions of the DC-6 aircraft are negligible. Since the boom may easily vibrate normal to its axis, but not along it, the transverse vibrations from the engines or aerodynamic forces should be considerably larger than similarly induced vibrations along the axis.

The magnitude of the velocity and temperature fluctuations in the range of interest is much smaller than the mean velocity and overheat temperature of the sensors. This permits King's law (1) to be linearized for each of the three anemometers to the form

$$\frac{2E_i'}{\bar{E}_i} = N\left(1 - \frac{A_i R_i \overline{\Delta T_i}}{\overline{E_i^2}}\right)\frac{u_i'}{\bar{U}_i} - \frac{\theta_i}{\overline{\Delta T_i}}, \quad i=1, 2, 3, \quad (2)$$

where an overbar denotes the mean or dc value, $\Delta T \equiv (T_w - T_a)$, U_i is the velocity component normal to the ith sensor, and $\theta \equiv T_a'$. A prime denotes $(x_i - \bar{x}_i)$, the fluctuating part of any quantity (x) using the Reynolds convention.

With the sensors and coordinates configured as in Fig. 6 the three anemometer signals may be written, using (2), as

$$\left.\begin{aligned} E_1' &= a_1(u'-w') - b_1\theta \\ E_2' &= a_2(u'+w') - b_2\theta \\ E_3' &= a_3 u' - b_3\theta \end{aligned}\right\}, \quad (3)$$

where the a_i and b_i are algebraic functions of $\bar{E}_i$, N, A_i, $\overline{\Delta T_i}$, $\bar{U}$. Another algebraic manipulation converts (3) into a set of the desired form

$$\left.\begin{aligned} u' &= \sum_{i=1}^{3} a_{ui} E_i' \\ w' &= \sum_{i=1}^{3} a_{wi} E_i' \\ \theta &= \sum_{i=1}^{3} a_{\theta i} E_i' \end{aligned}\right\}. \quad (4)$$

These equations are suitable for straightforward analog computation. For each data set the values of the a_{xi} are calculated from the calibration curves and operating conditions. Table 1 presents the values obtained for each tape.

TABLE 1. Coefficients [Eq. (4)] for u', w' (m s^{-1}) and θ (°C) given E_i' (V) after 40 dB amplification and recoloring.

Coefficient	Tape 14	Tape 15	Tape 16	Tape 17
a_{u1}	2.19	1.579	1.472	1.564
a_{u2}	2.52	1.914	1.776	1.910
a_{u3}	−5.26	−3.002	−2.748	−2.954
a_{w1}	−0.618	−0.577	−0.580	−0.590
a_{w2}	1.018	0.996	0.956	1.019
a_{w3}	−0.486	−0.419	−0.372	−0.424
$a_{\theta 1}$	0.483	0.325	0.303	0.302
$a_{\theta 2}$	0.556	0.393	0.365	0.368
$a_{\theta 3}$	−1.766	−1.108	−1.059	−1.045

The quantities resulting from (4) must be corrected for the peculiar frequency response of the probes due to the thermal properties of their substrate, and for the effect of pre-record prewhitening, both shown in Fig. 7. Correction for the frequency response of the probes is done manually following spectral processing. Removal of the effect of prewhitening (recoloration) is accomplished prior to spectral analysis using circuitry

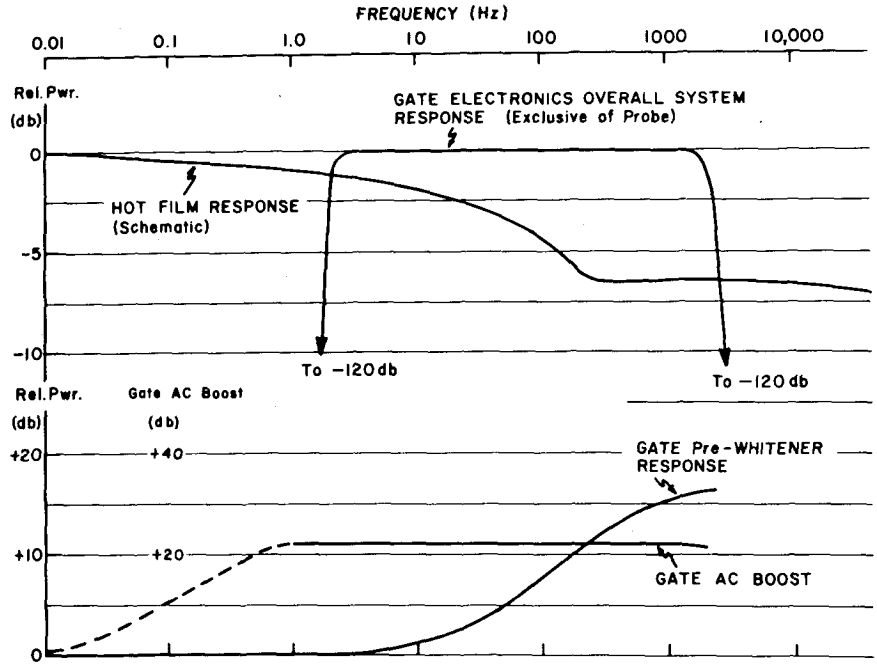

FIG. 7. Frequency responses of GATE system components.

which is the analog inverse of the prewhitening circuitry as shown in Fig. 8. In the same analog computer which recolors the data, the accelerometer signal can be used to compensate for the motion of the probes if necessary. Before Reynolds stresses, heat fluxes or spectra can be computed, the signals resulting from raindrop impacts must be removed from the data, and the record length corrected accordingly. These were also done with the analog computer.

5. Flight operations: Hardware performance

A major drawback to hot-sensor anemometry for airborne applications has been the supposed fragility of the sensors. The GATE experiment showed this drawback to be less serious than we had expected, except when heavy concentrations of Saharan dust were present. The mean lifetime of our probes was about 20 flight hours. Calibrations of probes before and after 16 flight hours in heavy dust agreed within 25%. During an 8 h flight where the dust concentration was low, calibration remained unchanged to within the limit of our ability to check it, i.e., to better than 1%. Based upon this experience, a mean lifetime of more than 60 h in dust-free areas would be a realistic expectation. In the absence of dust erosion, calibration can usually be expected to remain stable for at least 10 h, and for longer periods in many cases.

A chronic problem was the maintenance of an adequate signal-to-noise ratio. In addition to the grounding and cable reliability problems usually attending aircraft instrumentation, HF communications from the aircraft radio caused spurious signals at the anemometer outputs. Fortunately, radio silence was usually maintained on HF during data legs of the GATE flights. The internal noise level of the anemometers increased dramatically near the end of many missions. This was finally traced to the effect of prolonged exposure to the overheated environment in the aircraft and can be prevented by adequate ventilation and cooling of the equipment.

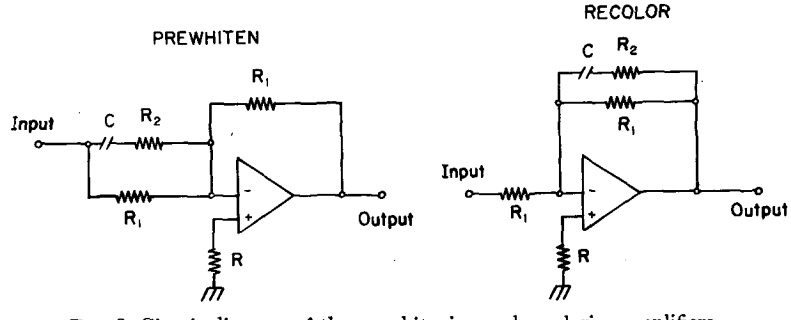

FIG. 8. Circuit diagram of the prewhitening and recoloring amplifiers.

A more serious signal-to-noise problem arose because we removed 20 dB of gain from the amplification system before recording the data for many of the flights. This turned out to have been a mistake. With the amplification in the system, we had signal-to-noise ratio ranging from 15 to 30 dB. Without it, the signal-to-noise ratio ranged from -5 to $+10$ dB. Fortunately, we got most of the data we sought during the brief period when the proper amplification was installed. The data presented below are from tapes made with an adequate signal-to-noise ratio.

6. System performance in clear air

Fig. 9 shows the noise spectrum of a single channel of the system before Eq. (4) is applied to separate temperature and velocity component signals. It includes all noise sources in the system. The figure also shows typical signal spectra at $Z=150$ m from a pair of single channels before component separation. The latter data were selected to show the different spectral densities and slopes generally encountered in processing signals from anemometers using different overheat ratios and having outputs compounded of several variables. The noise spectra of the three anemometers were invariant

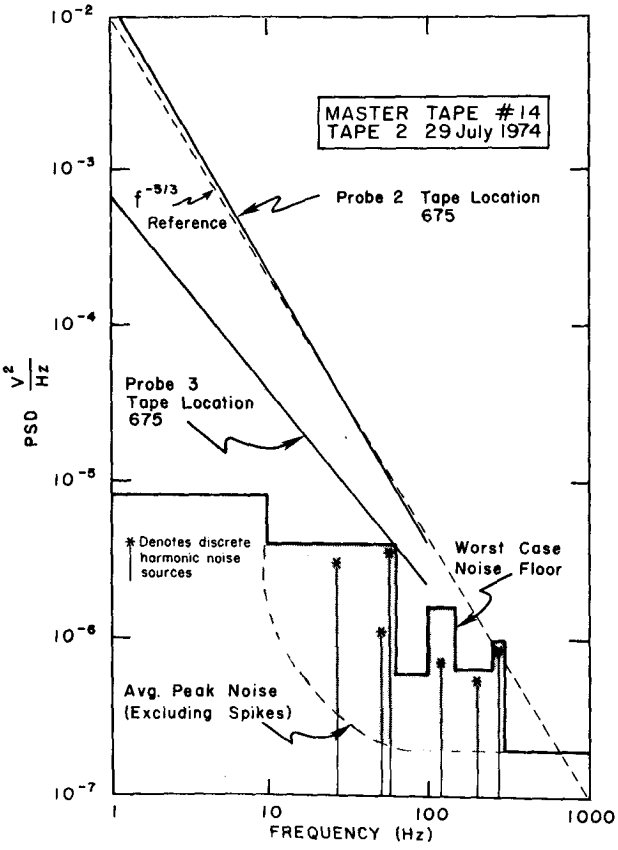

FIG. 9. Noise and clear air signal spectra of the hot-film system on playback from the data recorder.

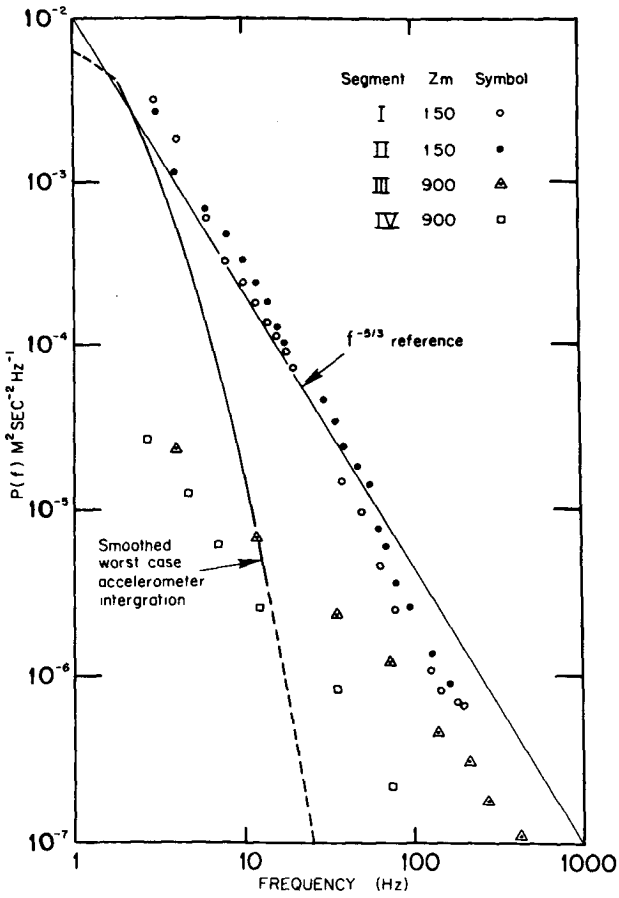

FIG. 10. Vertical velocity spectra from the anemometers and accelerometer.

and nearly identical, and dominated other noise sources except for power harmonics at multiples of 60 and 400 Hz and except for sources in the tape recorder. In plotting turbulence spectra, points falling on the offending discrete noise peaks have been omitted. The signal levels and slopes depend strongly on the environment, and a wide range of both was observed during the GATE exercise.

Fig. 10 shows vertical velocity spectra superimposed on a worst case accelerometer integration spectrum. The accelerometer spectrum (integrated to vertical velocity) represents the motion of the boom in wake turbulence behind a DC-7. It is two orders of magnitude larger than that typically encountered. The vertical velocity spectra at $Z=150$ m are typical of spectra at that altitude. The spectra at 900 m represent some of the lowest signal levels observed—the signal-to-noise ratio was marginal. Note that even the low-intensity spectra appear to be uncontaminated by boom vibration under normal circumstances. Figs. 11 and 12 show the horizontal velocity and temperature spectra corresponding to the w' spectra of Fig. 10 at 150 m. While inertial subrange ($f^{-\frac{5}{3}}$) behavior was most frequently observed, it is worth noting here that we also observed spectral char-

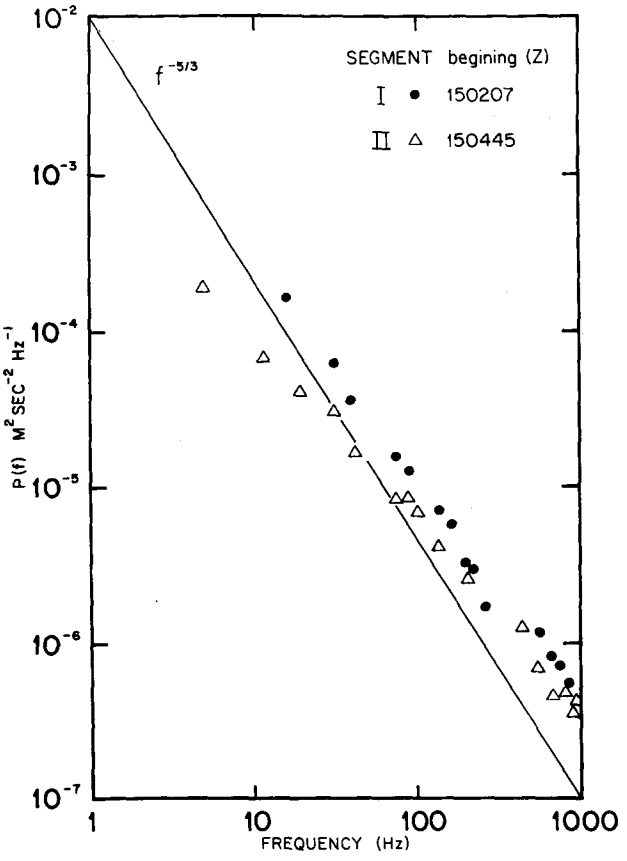

FIG. 11. Horizontal velocity spectra corresponding to the vertical spectra of Fig. 10.

acteristics which were not of that type, including buoyant subrange behavior (Lumley and Panofsky, 1964, p. 87) in a few places.

Dissipation rates ($cm^2\ s^{-3}$) corresponding to the velocity spectra shown in Fig. 10 are roughly 10 (150 m) and 0.01 (900 m), the latter being obtained in the inversion under suppressed conditions. The turbulence level in the atmosphere was large enough that an adequate signal-to-noise ratio was reliably obtained over the range from 2 Hz to >1000 Hz for altitudes up to at least 2000 m in areas of active convection and to at least 200 m in suppressed areas. The dissipation rates observed here in the tropical maritime boundary layer are consistent with those reported under similar conditions by other investigators [For example, Pennell and LeMone (1974) report $\epsilon = 20\ cm^2\ s^{-3}$ at $Z = 100$ m and $\epsilon = 8\ cm^2\ s^{-3}$ at $Z = 200$ m; see also Lumley and Panofsky, (1964, Chap. 4)]. However there is little in the literature to compare them with at the higher altitudes, although Pennell and LeMone (1974) report $\epsilon < 2\ cm^2\ s^{-3}$ at 600 m. The boom vibration was usually negligible at all altitudes, being down at least 10 dB except in a few extreme cases and often more than 20 dB at every frequency.

7. System performance within clouds

As expected, the system did not work well within clouds. Droplet impacts were too frequent to permit their separation from the turbulence signals.

8. System performance in subcloud rain

Except for the characteristic spikes in the signals betraying each raindrop impact as described by Merceret (1970), there is no difference between the performance of the system in subcloud rain and its performance in clear air. As long as the turbulence level is above the noise, which it usually seems to be, the anemometers will measure it accurately.

In rain, the major concern is the fraction of the record lost due to raindrop impacts on one or more of the probes. If T is the length of a record and T_R the portion of the record occupied by raindrop signals, then we may define the duty cycle δ of the data for the record as

$$\delta = \frac{T - T_R}{T}. \tag{5}$$

The closer δ is to unity, the smaller the loss of information. As δ approaches zero, the loss of information be-

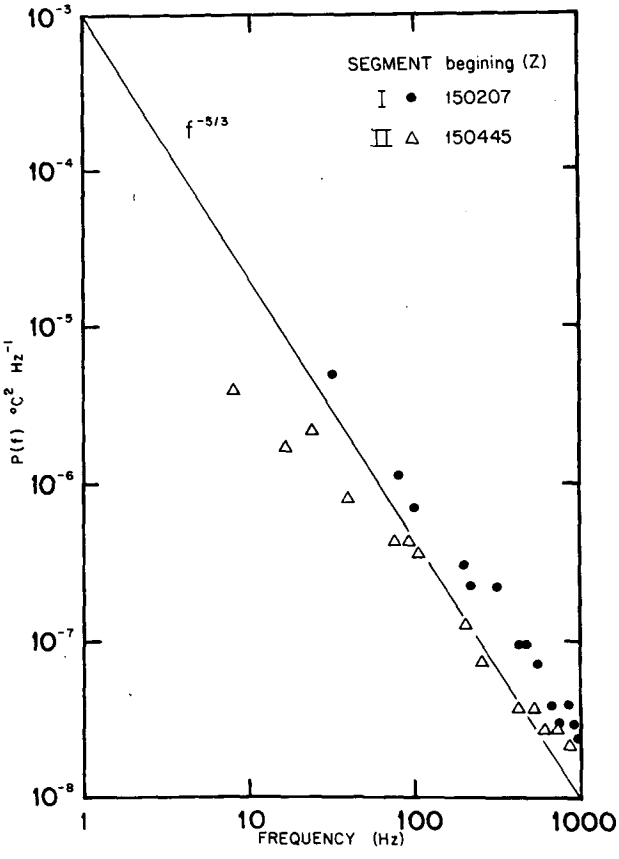

FIG. 12. Horizontal temperature spectra corresponding to the vertical spectra of Fig. 10.

comes total. For most statistical analysis, including correlation and spectral analysis, $\delta \geq 0.8$ will limit the error induced by the loss of record to $\leq 10\%$ if the raindrop spikes are randomly distributed. The loss is due to reduction of the effective sample size and can be overcome by analyzing longer records if the flow field is sufficiently stationary and homogeneous (e.g., Bendat and Piersol, 1966, Chaps. 5, 6, 7, 9). In rainfall as heavy as 30 mm h^{-1} we recorded impacts no more often than one every 10 s or so. The low impact rate, for which $\delta \approx 1$, indicates that the system can provide useful measurements in rainfall rates at least as great as 40 mm h^{-1} with no increase in record length over that required in clear air, and it will work in rainfall at least as heavy as 80 mm h^{-1} if the record length can be doubled. This should permit the measurement of fluxes and energy dissipation in the subcloud layer of tropical and other storms of moderate to severe rainfall intensity.

TABLE 2. Largest change (%) in the coefficients of Table 1 [Eq. (4)] for a 10% change in calibration parameters [Eq. (3)] to which each coefficient is most sensitive.

Coefficient	Tape 14	Tape 15	Tape 16	Tape 17
a_{u1}	23	15	15	15
a_{u2}	23	18	16	17
a_{u3}	30	23	22	22
a_{w1}	20	16	15	15
a_{w2}	21	18	16	17
a_{w3}	138****	71***	52**	67*
$a_{\theta 1}$	36	30	24	25
$a_{\theta 2}$	36	26	24	25
$a_{\theta 3}$	30	23	21	22

* Response to a_2; response to b_2 is 50%, all others <25%.
** Response to b_2; response to b_1 is 40%, all others <25%.
*** Response to a_2; response to b_2 is 52%, b_1 37%, all others <25%.
**** Response to a_2. Response to b_1 is 99%, b_2 79%, all others <25%.

9. Error sources in data reduction and limitations on the utility of the system

There are two principal error sources peculiar to this system: the frequency response characteristics of the probes and the sensitivity of (4) to variation of the coefficients in (3).

Because we did not have precisely matched probes, we have been able to frequency-compensate our signals at a given frequency only to within ± 1 dB. This results in up to 1 dB of error in the output of any variable. Although this sounds small, it represents a 25% error, enough, for example, to destroy any attempt to detect deviations from local isotropy by examining the ratio of w' spectra to u' spectra.

Similarly, because we used equipment with inadequate built-in calibration sources, we had uncertainties of as much as 5% in the coefficients in (3). Sensitivity tests presented in Table 2 show that this could change the values of the output variables by nearly 10% and the values of their spectra by 20%. The vertical component was found to be particularly subject to error in the coefficient of E_3' if there were any errors in determining a_2, b_1 or b_2. While a_2 was always known to within about 2%, the values of b_1 and b_2 were only known to within about 5%. This could result in as much as 70% error in the coefficient a_{w3} and lead to significant cross contamination of the w signal by u' and θ from probe 3. Since Table 2 presents the magnitude of worst case values and since the errors in the coefficients have random signs as well as magnitudes, the actual contamination in any given run will generally be smaller than that suggested by Table 2. It is not possible to tell *how much* smaller without more information than we have, but clearly the contamination will be significant for cross-spectral calculations.

As the system stands now, our best estimate is that we can measure spectra to within about $\pm 20\%$ and thereby estimate dissipation to within 30%, and accurately measure intermittency. The contamination of one velocity component by another because of the errors discussed above amounts to about 5% for u' and θ and may be somewhat larger for w'. This is large enough that cross spectra and correlations cannot be usefully computed until these errors are minimized by further work. The proper technique is to use matched probes and state-of-the-art anemometers with internal calibration facilities. With such components, accuracies of 1% or better seem well within reach. It would also be useful to tie the turbulence system into the aircraft's inertial navigation system so as to be able to measure the longer wavelength fluctuations which affect the motion of the aircraft. The system described in this paper measures a spectral region containing only a few percent of the energy in the turbulence field. This is fine for dissipation work but unacceptable for flux measurements. With anemometers of greater precision and extended low-frequency response, an upgraded hot-film system would be of significantly greater value than one limited to the accuracies and spectral regions presented here.

10. Conclusion

Hot-film anemometry can be a useful tool in the search for knowledge of the kinetic energy, momentum and heat balance of the atmosphere and its storms. With an additional sensor for the v component of the flow, better anemometers, and an interface with the aircraft's inertial navigation system, an upgraded version of the system described here should be able to measure the nine components of the Reynolds stress tensor and the three components of the heat flux vector over scales ranging from those of the mean flow to less than a centimeter. These measurements should be possible in clear air or in rain at any altitude. Flights into

ice will damage the probes, but flights into clouds are harmless (although data cannot be recovered in clouds due to the large number of droplets present).

Because the equipment required is readily available from several manufacturers the prompt introduction of this technique is possible wherever turbulence measurements are required.

Acknowledgments. The author thanks John Cunning, James DuGranrut and James G. McRory for operating the equipment aboard the aircraft. The use of the wind tunnel at the School of Engineering and Environmental Design, the University of Miami, is deeply appreciated. The figures for the manuscript were prepared by Dale Martin and Charlie True. This project was funded by the U. S. GATE Project Office and the National Hurricane Research Laboratory (now National Hurricane and Experimental Meteorology Laboratory), NOAA.

REFERENCES

Bendat, J. S., and A. G. Piersol, 1966: *Measurement and Analysis of Random Data.* Wiley, 390 pp.

Brown, W. J., Jr., J. D. McFadden, H. J. Mason, Jr., and C. W. Travis, 1974: Analysis of the Research Flight Facility gust probe system. *J. Appl. Meteor.*, **13**, 156–167.

Champagne, F. H., and C. A. Sleicher, 1967: Turbulence measurements with inclined hot-wires, Part 2. *J. Fluid Mech.*, **28**, 177–182.

Chernikov, A. A., Yu V. Mel'nichuk, N. Z. Pinus, S. M. Shmeter and N. K. Vinnichenko, 1969: Investigations of the turbulence in convective atmosphere using radar and aircraft. *Radio Sci.*, **4**, 1257–1259.

Corrsin, S., 1963: Turbulence: Experimental methods. *Handbuch der Physik*, Vol. VIII/2, Springer Verlag, 525–590.

Dorman, C. E., and E. Mollo-Christensen, 1973: Observation of the structure on moving gust patterns over a water surface ("cat's paws"). *J. Phys. Oceanogr.*, **3**, 120–132.

Hinze, J. O., 1959: *Turbulence.* McGraw Hill, 586 pp.

Kovasznay, L. S. G., 1965: The hot-wire anemometer. *Acta Tech. Acad. Sci. Hung.*, **50**, 131–151.

Lumley, J. L., and H. A. Panofsky, 1964: *The Structure of Atmospheric Turbulence.* Wiley, 239 pp.

Merceret, F. J., 1970: On the use of hot-film anemometry to measure turbulence in the presence of heavy rain. *J. Appl. Meteor.*, **19**, 191–193.

Pennell, W. T., and M. A. LeMone, 1974: An experimental study of turbulence structure in the fair-weather trade wind boundary layer. *J. Atmos. Sci.*, **31**, 1308–1323.

Pond, S., R. W. Stewart and R. W. Burling, 1963: Turbulence spectra in the wind over waves. *J. Atmos. Sci.*, **20**, 319–324.

Sheih, C. M., H. Tennekes and J. L. Lumley, 1971: Airborne hot-wire measurements of the small-scale structure of atmospheric turbulence. *Phys. Fluids*, **14**, 201–215.